Design of a Flapping Wing Mechanism to Coordinate Both Wing Swing and Wing Pitch

Peter L. Wang

Robotics and Automation Laboratory, University of California, Irvine, CA 92697 e-mail: wangpl1@uci.edu

J. Michael McCarthy

Robotics and Automation Laboratory, University of California, Irvine, CA 92697 e-mail: jmmccart@uci.edu

This paper presents a design procedure to achieve a flapping wing mechanism for a micro-air vehicle that coordinates both the wing swing and wing pitch with one actuator. The mechanism combines a planar four-bar linkage with a spatial four-bar linkage attached to the input and output links forming a six-bar linkage. The planar four-bar linkage was designed to control the wing swing trajectory profile and the spatial four-bar linkage was designed to coordinate the pitch of the wing to the swing movement. Tolerance zones were specified around the accuracy points, which were then sampled to generate a number of design candidates. The result was 29 designs that achieve the desired coordination of wing swing and pitch, and a prototype was constructed. [DOI: 10.1115/1.4038979]

1 Introduction

Flapping wing micro-air vehicles are winged aircraft generally smaller than 15 cm that mimic insect flight. The wings of these aircraft generally swing in a planar path without control of the wing pitch angle. This pitch angle is set by air drag forces that shape a membrane that forms the wing. See, for example, the aerovironment nanohummingbird [1].

Recent research by Taha et al. [2,3] shows that coordinating the wing pitch angle with the wing swing movement improves flight aerodynamics. This paper presents the synthesis procedure for a one degree-of-freedom flapping wing mechanism that coordinates the wing swing and pitch angles to achieve a specified performance.

This new flapping wing mechanism uses a spatial four-bar linkage to control the wing pitch that is built on a planar four-bar linage that controls the swing movement. The result is a six-bar mechanism, Fig. 1, that uses a single input to coordinate both the wing swing and pitch angles.

In what follows, we present the design methodology, solve for an example design, and present a prototype for this flapping wing mechanism.

2 Literature Review

The aerovironment nanohummingbird [1], and the Harvard RoboBee [4] have created flying flapping wing micro-air vehicle's whose wings pitch due to the aerodynamic drag induced by the wing's planar swinging motion. Our design provides a linkage, which coordinates both the wing's swing and pitch follow specific

Manuscript received September 22, 2017; final manuscript received December 6, 2017; published online January 29, 2018. Assoc. Editor: Andrew P. Murray.

functions. Yan et al. [5], Conn et al. [6], and Balta et al. [7] use parallel four-bar linkages and a spatial linkage to coordinate the swing and pitch of the wing, while we achieve this using a single six-bar mechanism. Recently, the Robo Raven [8] and the Bat Bot [9] have utilized a different flying mode in which extreme deformation of large wings is used to achieve flight.

A four-bar linkage that coordinates input and output angles is known as a function generator, Svoboda [10] and Freudenstein [11]. In our case, this linkage transforms a constant rotation of an input crank to an oscillating swing movement of the wing. The synthesis theory for function generators of this type is given by Brodell and Soni [12].

The control of the wing pitch is achieved by an RSSR function generator, see Denavit and Hartenberg [13] and Suh and Radcliffe [14]—R denotes a revolute or hinged joint and S denotes a spherical or ball joint. Our design approach uses the specified angle data to position the input and output cranks of the spatial four-bar linkage, and then solves the constraint equations for the SS link that connects the two, as described by Innocenti [15] and McCarthy and Soh [16].

The connection of the input and output links of a planar four-bar linkage with a spatial RSSR linkage creates a spatial six-bar linkage. The synthesis of spatial six-bar linkages has focused on the control of end-effector position and orientation rather than function generation. See, for example, Sandor et al. [17], who designed an RSSR-SS spatial six-bar and Chiang et al. [18], who designed an RSCC-RRS spatial six-bar, where C denotes a cylindric joint. Recent research includes the design of a spatial six-bar linkage to guide the end effector to trace a spatial path, see Chung [19].

This paper is the first to explore the use of a spatial six-bar linkage to coordinate two outputs to a given input.

3 Wing Swing and Wing Pitch Requirements

A study of flapping wing designs for micro-air vehicles [7] shows that planar crank-rocker linkages with a passive position of the wing pitch provide effective wing performance. However, Yan et al. [20] show that coordinated control of the wing pitch and wing swing movement improves the aerodynamics of a micro-air vehicle.

They demonstrate effective aerodynamic performance with wing swing and wing pitch functions, $q(\theta)$ and $\phi(\theta)$, given by

$$q(\theta) = \frac{\pi}{2} - \frac{\pi}{3}\cos\theta, \quad \phi(\theta) = \frac{\pi}{2} - \frac{\pi}{3}\sin\theta \tag{1}$$

where the driving angle is $\theta = \omega t$, and ω is the flapping frequency, Fig. 2.

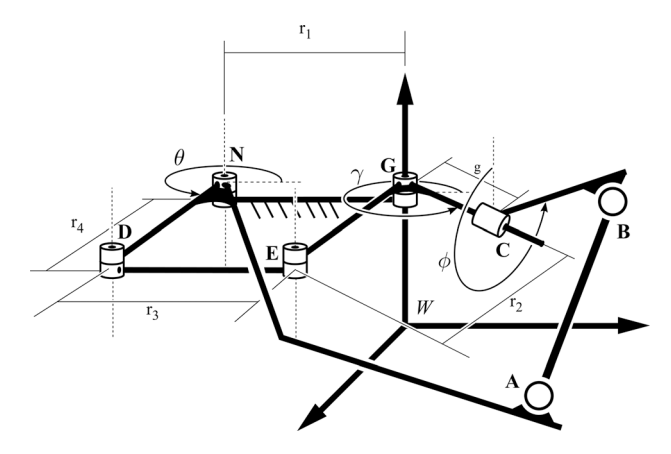


Fig. 1 The six-bar mechanism is composed of the spatial RSSR and planar four-bar mechanisms. The frames of reference used to define the rotation axes are shown.

Journal of Mechanisms and Robotics

Copyright © 2018 by ASME

APRIL 2018, Vol. 10 / 025003-1

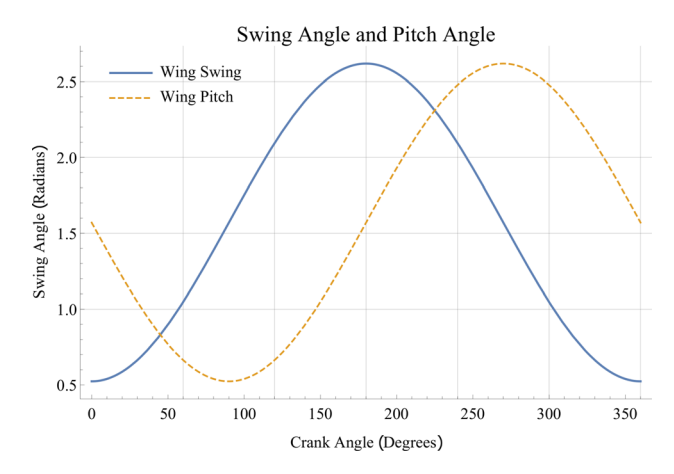


Fig. 2 The wing swing and wing pitch functions

4 Synthesis of the Wing Swing Mechanism

In order to design the wing swing mechanism, we follow Brodell and Soni [12] to obtain a four-bar linkage that has a time ratio of one. This ensures the speed of the flapping movement is the same in both the forward and back strokes.

Brodell and Soni provide formulas for the link lengths parameterized by the desired wing swing angle σ and transmission angle λ

$$\frac{r_3}{r_1} = \sqrt{\frac{1 - \cos \sigma}{2 \cos^2 \lambda}}, \quad \frac{r_4}{r_1} = \sqrt{\frac{1 - (r_3/r_1)^2}{1 - (r_3/r_1)^2 \cos^2 \lambda}},
\frac{r_2}{r_1} = \sqrt{\left(\frac{r_3}{r_1}\right)^2 + \left(\frac{r_4}{r_1}\right)^2 - 1}$$
(2)

where r_1 , r_2 , r_3 , and r_4 are the lengths of the ground link, the input crank, the coupler link, and the follower link, respectively.

Given the link lengths of the crank rocker, the wing swing function $\gamma(\Delta\theta)$ where $\Delta\theta$ is measured from the line **NG** of the linkage [16]

$$A(\Delta\theta)\cos\gamma + B(\Delta\theta)\sin\gamma = C(\Delta\theta) \tag{3}$$

where

$$A(\Delta\theta) = 2r_2r_4\cos\Delta\theta + 2r_1r_4, \quad B(\Delta\theta) = 2r_2r_4\sin\Delta\theta, C(\Delta\theta) = r_1^2 + r_2^2 + r_4^2 - r_3^2 + 2r_1r_2\cos\Delta\theta$$
 (4)

This has the solution

$$\gamma(\Delta\theta) = \arctan\left(\frac{B}{A}\right) \pm \arccos\left(\frac{C}{\sqrt{A^2 + B^2}}\right)$$
 (5)

Our goal is to achieve the four-bar linkage output $\bar{\gamma}(\theta) = \gamma(\theta_0 + \Delta\theta) + k_0$ that matches the wing swing function $q(\theta)$ at $\theta = 0$ and where $q(0) = \pi/6$ and the minimum of γ is at $\gamma(0.045) = 0.568$. Thus, $0 = \theta_0 + 0.045$ and $\pi/6 = 0.568 + k_0$. The result is $\theta_0 = -0.045$ or $-2.6 \deg$ and $k_0 = -0.045$ or $-2.6 \deg$, as seen in Fig. 3.

Thus, we obtain

$$\bar{\gamma} = \gamma(\Delta\theta - 0.045) - 0.045 \tag{6}$$

5 Synthesis of the Pitch Mechanism

In order to control the pitch of the flapping wing, we introduce an RSSR linkage connecting the input and output links of the swing mechanism that will orient the pitch of the wing during the flapping movement.

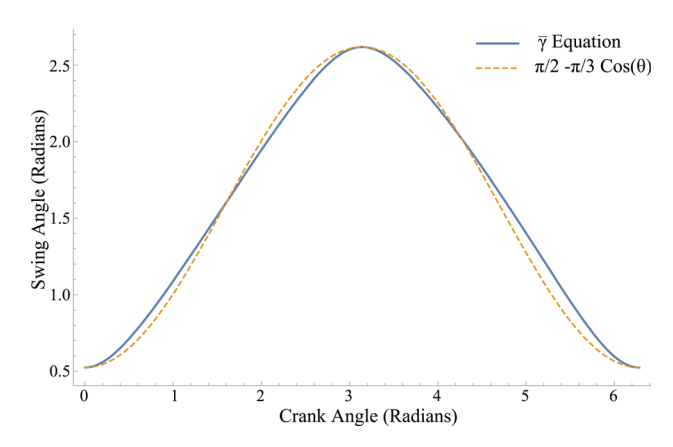


Fig. 3 Comparison of the task swing function $q(\theta)$ and the output of the swing mechanism $\bar{\gamma}(\theta)$

The planar wing swing mechanism **NDEG**, shown in Fig. 1, is positioned in the ground frame W such that the fixed pivot G of the link **EGC** is on the z-axis of W. The axes of the four joints of the planar four-bar **NDEG** are also directed along the z-axis of W. The rotation γ of **EGC** provides the swing of the wing. The output crank **CB** of the RSSR linkage **NABC** controls the pitch ϕ of the wing around the axis of G. The output of the wing swing mechanism **NDEG** is an input to the wing pitch mechanism **NABC**. The dimension G is selected by the designer.

The location of the fixed pivot $\mathbf{N} = (0, t, 0)$ of input crank **DNA** is selected by the designer so that the ground link **GN** has the length r_1 . The input rotation of **DNA** about the axis of **N** drives both the planar wing swing mechanism and spatial wing pitch mechanism.

Our goal is to determine the dimensions of the linkage by solving the SS constraint equations for seven values of the wing pitch function, $\phi_i = \phi(\theta_i)$, i = 1, ..., 7, see Ref. [16]. The values, $\phi(\theta_i)$, are chosen using Chebyshev spacing along the wing pitch function [21].

The synthesis equations coordinate the rotation of the link **DNA**, **EGC**, and **BC** links so that they simultaneously satisfy, $\bar{\gamma}_i = \bar{\gamma}(\theta_i)$ and $\phi_i = \phi(\theta_i)$, i = 1, ..., 7.

The homogeneous transforms Z and X that define coordinate screw displacement about the x- and z-axes, given by

$$\mathbf{Z}(\theta, d) = \begin{bmatrix} \cos \theta & -\sin \theta & 0 & 0\\ \sin \theta & \cos \theta & 0 & 0\\ 0 & 0 & 1 & d\\ 0 & 0 & 0 & 1 \end{bmatrix},$$

$$\mathbf{X}(\alpha, a) = \begin{bmatrix} 1 & 0 & 0 & a\\ 0 & \cos \alpha & -\sin \alpha & 0\\ 0 & \sin \alpha & \cos \alpha & 0\\ 0 & 0 & 0 & 1 \end{bmatrix}$$
(7)

are used to locate the axis of rotation of N for the input to the RSSR linkage and the axis of C for the output, Fig. 1.

The rotation axis of N of the input crank DNA is defined by the sequence of transformations

$$\mathbf{H}(\theta) = \mathbf{X}(0, t)\mathbf{Z}(\theta, 0) \tag{8}$$

where the parameter θ defines the rotation of the link **DNA** and (0,t) defines its position relative to the ground frame, see Fig. 1. Let \mathbf{H}_{i1} be the transformation relative to the initial configuration of the RSSR chain evaluated at seven task angles θ_i , i=1,...,7, so we have

$$\mathbf{H}_{i1} = \mathbf{H}_i \mathbf{H}_1^{-1}, \quad i = 1, ..., 7$$
 (9)

Transactions of the ASME

025003-2 / Vol. 10, APRIL 2018

The rotation axis of ${\bf C}$ of the output crank ${\bf CB}$ is defined by the sequence of transformations

$$\mathbf{J}(\phi, \bar{\gamma}) = \mathbf{Z}(\bar{\gamma}, 0)\mathbf{X}(\pi/2, 0)\mathbf{Z}(\phi, g) \tag{10}$$

where $\bar{\gamma}$ and g define the position relative to the ground frame, and ϕ defines the rotation of the output crank. Let \mathbf{J}_{i1} denote the transformation relative to the initial configuration of the RSSR chain evaluated at seven task angles ϕ_i , i = 1, ..., 7

$$\mathbf{J}_{i1} = \mathbf{J}_i \cdot \mathbf{J}_1^{-1} \quad i = 1, ..., 7$$
 (11)

The design equations for wing pitch mechanism are obtained as the constraint that the length of the SS link be constant in each of the task positions specified by $\phi_i = \phi(\theta_i)$, i = 1, ..., 7. Let the coordinates of the centers **A** and **B** of the S-joints in the first task position be given by

$$\mathbf{A}^1 = (u, v, w), \quad \mathbf{B}^1 = (x, y, z)$$
 (12)

Then the constraint that the coupler link AB is of constant length b = |AB| in each of the task positions yields the equations

$$|\mathbf{A}^{i} - \mathbf{B}^{i}|^{2} = |([\mathbf{H}_{i1}]\mathbf{A}^{1} - [\mathbf{J}_{i1}]\mathbf{B}^{1})|^{2} = b^{2}, \quad i = 1, ..., 7$$
 (13)

These equations can be reduced to a degree 20 polynomial in terms of one of the following u, v, w, x, y, or z, [15,16], and thus the system of equations has a maximum of 20 unique solutions. This set of equations was solved using Mathematica, which yielded values for the points $\mathbf{A}^1 = (u, v, w)$ and $\mathbf{B}^1 = (x, y, z)$. The solutions found are all possible solutions for the set of specified dimensions and angles.

6 Analysis of the Wing Pitch Mechanism

In order to evaluate the linkage obtained from the synthesis routine, we analyze RSSR Wing pitch mechanism at each input crank position. The goal is to verify that the mechanism moves smoothly through the specified wing swing and wing pitch movements. Every solution from the synthesis is analyzed.

The constraint equation of the RSSR chain defining the length of the link **AB** in terms of $\Delta\theta$, $\bar{\gamma}$, and ϕ is given by

$$|[\mathbf{H}(\Delta\theta)]\mathbf{a} - [\mathbf{J}(\phi,\bar{\gamma})]\mathbf{b}|^2 = b^2$$
 (14)

where ${\bf H}$ and ${\bf J}$ are given in Eqs. (8) and (10) and ${\bf a}$ and ${\bf b}$ are the coordinates of ${\bf A}^1$ and ${\bf B}^1$ in the frame of the first task position given by

$$\mathbf{a} = [\mathbf{H}_1]^{-1} \mathbf{A}^1 = (\bar{u}, \bar{v}, \bar{w}), \quad \mathbf{b} = [\mathbf{J}_1]^{-1} \mathbf{B}^1 = (\bar{x}, \bar{y}, \bar{z})$$
 (15)

For each value of $\Delta\theta$, we obtain $\bar{\gamma}$, and obtain an equation of the form

$$A(\Delta\theta)\cos\phi + B(\Delta\theta)\sin\phi = C(\Delta\theta) \tag{16}$$

where

$$\begin{split} A(\Delta\theta) &= -2t\bar{x}\cos(\gamma) - 2\bar{u}\bar{x}\cos(\gamma - \Delta\theta) - 2\bar{v}\bar{x}\sin(\gamma - \Delta\theta) - 2\bar{w}\bar{y} \\ B(\Delta\theta) &= +2t\bar{y}\cos(\gamma) + 2\bar{u}\bar{y}\cos(\gamma - \Delta\theta) + 2\bar{v}\bar{y}\sin(\gamma - \Delta\theta) - 2\bar{w}\bar{x} \\ C(\Delta\theta) &= -b^2 + g^2 + t^2 + \bar{x}^2 + \bar{y}^2 + \bar{z}^2 + \bar{u}^2 + \bar{v}^2 + \bar{w}^2 \\ &\quad + 2g\bar{z} - 2gt\sin(\gamma) - 2g\bar{u}\sin(\gamma - \Delta\theta) \\ &\quad + 2g\bar{v}\cos(\gamma - \Delta\theta) + 2t\bar{u}\cos(\Delta\theta) - 2t\bar{v}\sin(\Delta\theta) \\ &\quad - 2t\bar{z}\sin(\gamma) - 2\bar{u}\bar{z}\sin(\gamma - \Delta\theta) + 2\bar{v}\bar{z}\cos(\gamma - \Delta\theta) \end{split} \tag{17}$$

where g and t are determined by the designer.

Solve for $\phi_i(\Delta \theta_i)$ i = 1, ..., 7 using Eq. (5).

The solutions that pass through all precision points on a single branch pass the branching analysis. The passing solutions are then

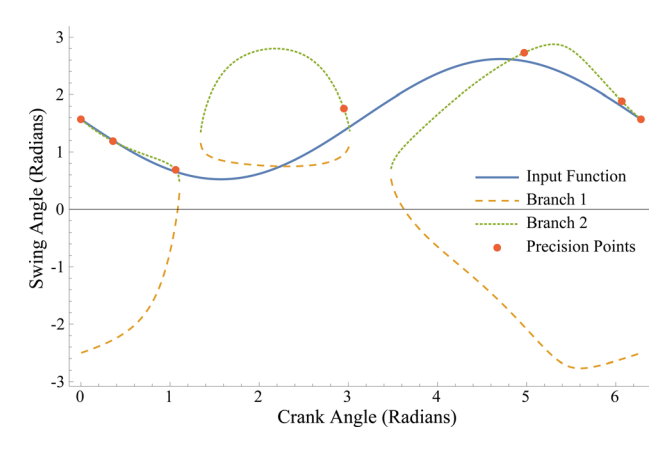


Fig. 4 The plot of a noncontinuous solution

checked for continuity. The range of the input crank angles is divided into 200 intermediate angles, and the links are checked to ensure that they do not change length at the intermediary positions. The solutions are plotted for the entire range of motion of the input crank. An example of a solution that fails in continuity but passes branching is shown in Fig. 4.

7 Design Methodology

Our design methodology consists of three steps: (i) the required wing swing movement is used to design a planar four-bar function generator; (ii) the coordinate wing pitch movement is used to formulate and solve the SS chain constraints for inverted task positions within specified tolerance zones; and (iii) each solution is analyzed to evaluate its continuous movement through the task positions. This process is iterated with randomly selected task positions within the tolerance zones. Successful design candidates are collected, ranked, and evaluated by the designer.

8 Example Flapping Wing Mechanism

The precision points of θ and ϕ were chosen by applying Chebyshev Spacing on Eq. (1). The calculated input crank angles(θ) are then substituted into the planar linkage equation, see Eq. (6), to obtain the wing swing angle $\bar{\gamma}$. The values of the tolerance zones for each precision point $\pm \delta \theta_i$ and $\pm \delta \phi_i$ are selected by the designer. The values are seen in Table 1.

The planar mechanism was chosen to have a total wing swing angle $\sigma = \pi/3$ from $q(\theta)$ in Eq. (5), a base length $r_1 = 5$, and a transmission angle of 0.521 deg or 29.9 deg. The corresponding values of r_2 , r_3 , and r_4 are seen in Table 2. These values are substituted into Eq. (5), which gives $\gamma(\theta)$ a minimum at $\gamma(0.045) = 0.568$ deg. Thus, $\theta_0 = -0.045$ or -2.6 deg and $k_0 = 0.045$ or 2.6 deg and the wing swing equation is

Table 1 Table of initial parameter angles for seven precision points

		Wing pitch angle requirements (rad)								
i	1	2	3	4	5	6	7			
θ_i	0	0.15	1.30	3.14	4.99	6.13	6.28			
$\delta\theta_i$	0	± 0.26	± 0.26	± 0.26	± 0.26	± 0.26	0			
ϕ_i	1.57	1.41	0.56	1.57	2.58	1.73	1.57			
$\delta \phi_i$	0	± 0.26	± 0.26	± 0.26	± 0.26	± 0.26	0			
$\bar{\gamma}_i$	0.52	0.54	1.34	2.62	1.41	0.55	0.52			

Journal of Mechanisms and Robotics

APRIL 2018, Vol. 10 / 025003-3

Table 2 Solution for planar crank rocker for given input parameters

Dimensions for planar linkage								
GN 5.00	ND 0.39	DE 4.99	EG 0.45	$\begin{array}{c} \theta_0 \\ -0.04 \end{array}$	$k_0 - 0.04$			

Table 3 Table of coordinate solutions

		Ranked design candidates								
				A coordinates			B coordinates			
	3	κ	и	v	w	х	у	z		
1	0.89	2.86	2.25	0.57	-3.32	-1.16	-1.22	-1.23		
2	1.39	2.92	7.64	-3.24	-4.31	2.73	0.12	1.67		
3	1.29	3.28	-7.06	-4.66	-4.14	1.21	-2.64	0.22		
4	1.37	3.42	-3.98	-1.87	-4.12	0.72	-1.72	0.47		
5	1.35	12.9	-6.42	-0.52	-5.46	0.15	0.05	-0.64		
6	1.03	16.6	-3.50	-0.02	-4.68	0.01	-0.19	0.31		

Table 4 Table of randomized input parameters

Selected task position for solution 4									
θ	0.	0.40	1.17	3.35	5.24	6.09	6.28		
ϕ	1.57	1.19	0.80	1.83	2.76	1.81	1.57		
γ	0.52	0.65	1.24	2.58	1.18	0.56	0.52		

$$\begin{split} \overline{\gamma}(\Delta\theta) &= \tan^{-1} \frac{2.24 - 0.17\cos(\Delta\theta + 0.04)}{-0.17\sin(\Delta\theta + 0.04)} \\ &+ \cos^{-1} \left(\frac{4.33\cos(\Delta\theta + 0.04) - 0.45}{\sqrt{0.17\sin\Delta\theta - 3.88\cos\Delta\theta + 25.15}} \right) - 0.04 \end{split}$$

To align the planar and spatial linkages, the input crank axis of the spatial linkage was placed such that t=-5 in and the output crank axis such that g=0. Knowing t,g,θ_i,ϕ_i and $\bar{\gamma}_i$ for $i=1,\ldots,7$ and solving Eq. (13) for (u,v,w,x,y,z) gives the coordinates of \mathbf{A}^1 and \mathbf{B}^1 in the global frame W. The θ_i values were selected in the range of $\pm \delta \theta_i$ and the ϕ_i values were selected in the range of $\pm \delta \phi_i$. The $\bar{\gamma}_i$ values were recalculated using Eq. (18) and the values of θ_i .

Five hundred variations produced 3582 solutions of which 29 met the design requirements. The 29 design candidates were sorted in ascending order by the link ratio κ , where $\kappa =$ (Longest Link Length/Shortest Link Length). The RMS error of ϵ between each of the top six results and desired wing pitch function of $\phi(\theta_k)$ given in Eq. (1) was calculated using

$$\varepsilon = \sqrt{\frac{\sum_{k=1}^{n} (\bar{\phi}(\theta_k) - \phi(\theta_k))}{n}}$$
(19)

where $\bar{\phi}(\theta_k)$ is the wing pitch function from the solution, and n is the number of samples.

Design number 1 was selected because it has the lowest RMS error of the designs with a link ratio less than 10, see Table 3. Results with link ratios less than 10 improved the ease of manufacturing. Its associated inputs are in Table 4 and the output is plotted in Fig. 5.

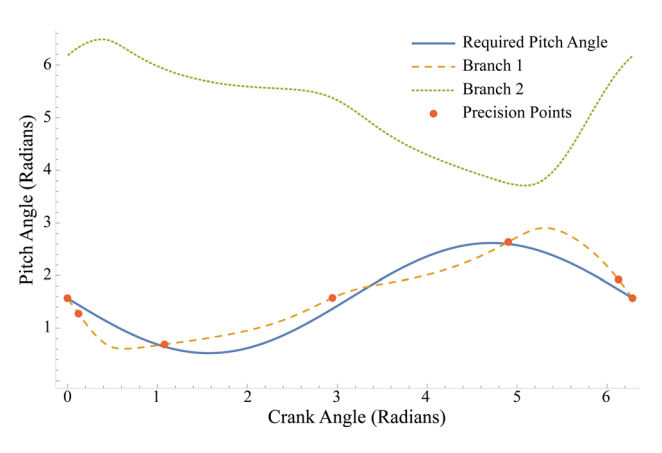


Fig. 5 The required pitch path versus selected pitch path

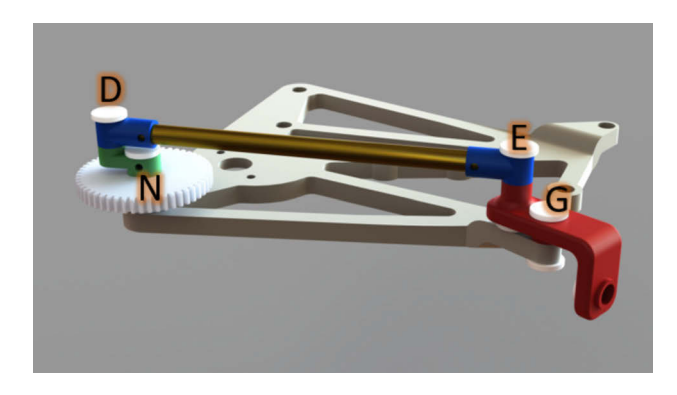


Fig. 6 The planar mechanism NGED

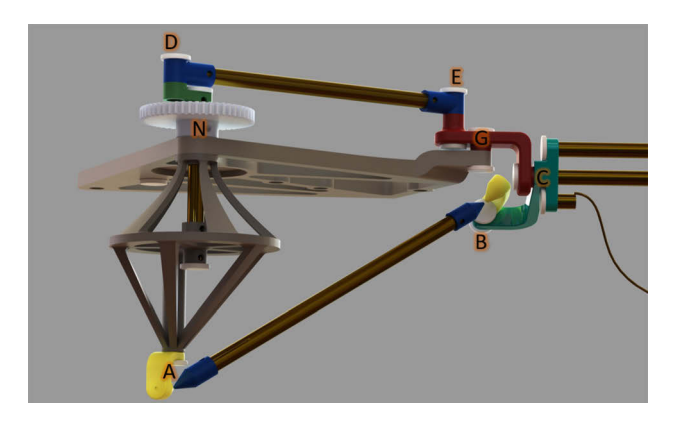


Fig. 7 Planar spatial flapping wing mechanism

The mechanism was modeled in SolidWorks, see Figs. 6–8. Figure 9 compares the SolidWorks output, the generated configuration output, and the required wing pitch angle. The SolidWorks model shows some discrepancy due to minor adjustments to the structure that allow it to be physically constructed. The dimensions used are shown in Table 5.

The physical model of the linkage was built, shown in Figs. 10 and 11. The wing span of the flapping mechanism is 34 in. The straight links and end caps were machined from aluminum or brass tubing. The remaining links and base were made from polycarbonate using additive manufacturing. The revolute joints used brass tubes as bushings while the spherical joints used a compliant joint that used a wire rope to connect the links. The right and left wings are driven by a gear train that connects a motor to their input cranks. The mechanism was driven at a rate of

025003-4 / Vol. 10, APRIL 2018

Transactions of the ASME

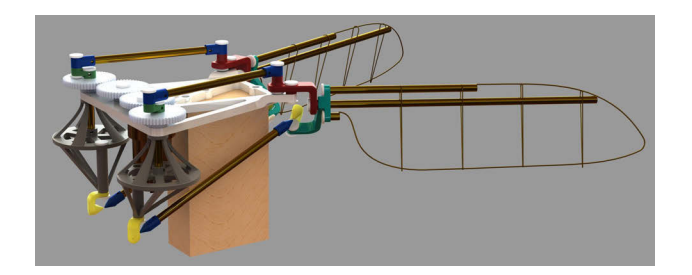


Fig. 8 Solid model of the full flapping wing assembly

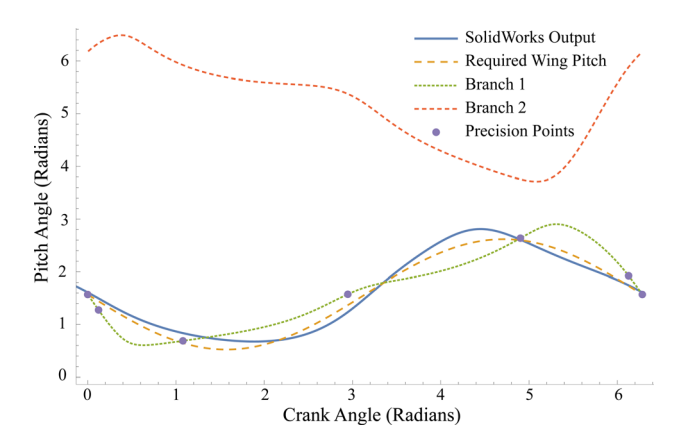


Fig. 9 The SolidWorks pitch angle versus required pitch path versus selected pitch path

Table 5 Table of link lengths for the spatial mechanism

Solution 4: dimensions for spatial linkage								
NA 4.48	AB 6.57	BC 1.44	CG 1.27	θ_s 2.70	ϕ_s 3.66			



Fig. 10 Physical model of the flapping wing mechanism

Journal of Mechanisms and Robotics



Fig. 11 Gear train and input cranks of the physical model of the flapping wing mechanism

approximately 2–3 Hz, but was not driven any faster due to its size. The focus of this model is to confirm the movement of the proposed linkage. Future research will pursue developing methods to miniaturize and construct a model with a wing span of 5 in.

9 Conclusion

This paper presents a design methodology for an RSSR mechanism built on the planar four-bar mechanism to coordinate the wing pitch angle with the swing movement of a flapping wing micro-air vehicle. The resulting mechanism is a spatial six-bar linkage that transforms a rotational input to coordinated wing pitch angle and swing angles. The design procedure is demonstrated for wing swing and wing pitch profiles recommended for micro-air vehicles. It results in 29 different designs that meet the requirements, one of which is presented in detail together with a prototype.

Acknowledgment

Benjamin Liu's preparation of the geometric models is gratefully acknowledged.

Funding Data

Division of Civil, Mechanical and Manufacturing Innovation (Grant No. 1636017).

References

- Keennon, M., Klingebiel, K., Won, H., and Andriukov, A., 2012, "Development of the Nano Hummingbird: A Tailless Flapping Wing Micro Air Vehicle," AIAA Paper No. 2012-0588.
- [2] Taha, H. E., Nayfeh, A. H., and Hajj, M. R., 2014, "Effect of the Aerodynamic-Induced Parametric Excitation on the Longitudinal Stability of Hovering Mavs/ Insects," Nonlinear Dyn., 78(4), pp. 2399–2408.
- [3] Taha, H. E., Tahmasian, S., Woolsey, C. A., Nayfeh, A. H., and Hajj, M. R., 2015, "The Need for Higher-Order Averaging in the Stability Analysis of Hovering Mavs/Insects," Bioinspiration Biomimetics, 10(1), p. 016002.
- [4] Ma, K., Chirarattananon, P., Fuller, S., and Wood, R., 2013, "Controlled Flight of a Biologically Inspired, Insect-Scale Robot," Science, 340(6132), pp. 603–607.
- [5] Yan, J., Avadhanula, S., Birch, J., Dickinson, M., Sitti, M., Su, T., and Fearing, R., 2001, "Wing Transmission for a Micromechanical Flying Insect," J. Micromechatronics, 1(3), pp. 221–237.
- [6] Conn, A. T., Burgess, S. C., and Ling, C. S., 2007, "Design of a Parallel Crank-Rocker Flapping Mechanism for Insect-Inspired Micro Air Vehicles," Proc. Inst. Mech. Eng., Part C, 221(10), pp. 1211–1222.
- [7] Balta, M., Ahmed, K. A., Wang, P. L., McCarthy, J. M., and Taha, H. E., 2017, "Design and Manufacturing of Flapping Wing Mechanisms for Micro Air Vehicles," AIAA Paper No. 2017-0509.
- [8] John, G., Alex, H., Ariel, P.-R., Luke, R., Adrian, G., Eli, B., Johannes, K., Deepak, L., Yeh, C.-H., Bruck, H. A., and Satyandra, G. K., 2014, "Robo Raven: A Flapping-Wing Air Vehicle With Highly Compliant and Independently Controlled Wings," Soft Rob., 1(4), pp. 275–288.
- [9] Ramezani, A., Chung, S.-J., and Hutchinson, S., 2017, "A Biomimetic Robotic Platform to Study Flight Specializations of Bats," Sci. Rob., 2(3), p. eaal2505.

APRIL 2018, Vol. 10 / 025003-5

- [10] Svoboda, A., 1948, Computing Mechanisms and Linkages, McGraw-Hill, New York.
 [11] Freudenstein, F., 1954, "An Analytical Approach to the Design of Four-Link Mechanisms," Trans. ASME, 76(3), pp. 483–492.
 [12] Brodell, R. J., and Soni, A., 1970, "Design of the Crank-Rocker Mechanism With Unit Time Ratio," J. Mech., 5(1), pp. 1–4.
 [13] Denavit, J., and Hartenberg, R. S., 1960, "Approximate Synthesis of Spatial Linkages," ASME J. Appl. Mech., 27(1), pp. 201–206.
 [14] Suh, C. H., and Radcliffe, C. W., 1978, Kinematics and Mechanisms Design, Wiley, New York.
 [15] Innocenti, C. 1995, "Polynomial Solution of the Spatial Burmester Problem."

- [15] Innocenti, C., 1995, "Polynomial Solution of the Spatial Burmester Problem," ASME J. Mech. Des., 117(1), pp. 64–68.
 [16] McCarthy, J. M., and Soh, G. S., 2010, Geometric Design of Linkages, Vol. 11,
- Springer Science & Business Media, New York.
- [17] Sandor, G. N., Xu, L. J., and Yang, S. P., 1986, "Computer-Aided Synthesis of Two-Closed-Loop RSSR-SS Spatial Motion Generator With Branching and Sequence Constraints," Mech. Mach. Theory, 21(4), pp. 345–350.
 Chiang, C. H., Yang, Y.-N., and Chieng, W. H., 1994, "Four-Position Synthesis for Spatial Mechanisms With Two Independent Loops," Mech. Mach. Theory, 21(2)
- [19] Chung, W.-Y., 2015, "Synthesis of Spatial Mechanism UR-2SS for Path Generation," ASME J. Mech. Rob., 7(4), p. 041009.
 [20] Yan, Z., Taha, H. E., and Hajj, M. R., 2015, "Effects of Aerodynamic Modeling
- on the Optimal Wing Kinematics for Hovering MAVs," Aerosp. Sci. Technol., **45**, pp. 39–49.
- [21] Hartenberg, R. S., and Denavit, J., 1964, Kinematic Synthesis of Linkages, McGraw-Hill, New York.